Manoyl Oxide (13R), the Biosynthetic Precursor of Forskolin, Is Synthesized in Specialized Root Cork Cells in *Coleus forskohlii*[1][W][OPEN]

Irini Pateraki[2], Johan Andersen-Ranberg[2], Britta Hamberger, Allison Maree Heskes, Helle Juel Martens, Philipp Zerbe, Søren Spanner Bach, Birger Lindberg Møller, Jörg Bohlmann, and Björn Hamberger*

Department of Plant and Environmental Sciences, Faculty of Science, University of Copenhagen, Thorvaldsensvej 40, 1871 Copenhagen, Denmark (I.P., J.A.-R., Br.H., H.J.M., S.S.B., B.L.M., Bj.H.); Center for Synthetic Biology bioSYNergy, 1871 Copenhagen, Denmark (J.A.-R., B.L.M., Bj.H.); School of Botany, University of Melbourne, Victoria 3010, Australia (A.M.H.); and Michael Smith Laboratories, University of British Columbia, Vancouver, British Columbia, Canada V6T 1Z4 (P.Z., J.B.)

ORCID IDs: 0000-0002-7526-2334 (I.P.); 0000-0002-3252-3119 (B.L.M.); 0000-0003-1249-1807 (B.H.).

Forskolin, a complex labdane diterpenoid found in the root of *Coleus forskohlii* (Lamiaceae), has received attention for its broad range of pharmacological activities, yet the biosynthesis has not been elucidated. We detected forskolin in the root cork of *C. forskohlii* in a specialized cell type containing characteristic structures with histochemical properties consistent with oil bodies. Organelle purification and chemical analysis confirmed the localization of forskolin and of its simplest diterpene precursor backbone, (13R) manoyl oxide, to the oil bodies. The labdane diterpene backbone is typically synthesized by two successive reactions catalyzed by two distinct classes of diterpene synthases. We have recently described the identification of a small gene family of diterpene synthase candidates (CfTPSs) in *C. forskohlii*. Here, we report the functional characterization of four CfTPSs using in vitro and in planta assays. CfTPS2, which synthesizes the intermediate copal-8-ol diphosphate, in combination with CfTPS3 resulted in the stereospecific formation of (13R) manoyl oxide, while the combination of CfTPS1 and CfTPS3 or CfTPS4 led to formation of miltiradiene, precursor of abietane diterpenoids in *C. forskohlii*. Expression profiling and phylogenetic analysis of the CfTPS family further support the functional diversification and distinct roles of the individual diterpene synthases and the involvement of CfTPS1 to CfTPS4 in specialized metabolism and of CfTPS14 and CfTPS15 in general metabolism. Our findings pave the way toward the discovery of the remaining components of the pathway to forskolin, likely localized in this specialized cell type, and support a role of oil bodies as storage organelles for lipophilic bioactive metabolites.

Coleus forskohlii (synonym: *Plectranthus barbatus*) is a perennial medicinal shrub of the mint family (Lamiaceae) indigenous to the subtropical and temperate climate zones of India and southeast Asia (Kavitha et al., 2010). The plant has been used since ancient times in Hindu and Ayurvedic traditional medicine for treating a broad range of human health disorders (Valdés et al., 1987; Lukhoba et al., 2006). The main active compound of *C. forskohlii* is forskolin, a heterocyclic labdane-type diterpene found in the roots of the plant (Ammon and Müller, 1985). The diverse known and potential pharmaceutical applications of forskolin extend from alleviation of glaucoma (Wagh et al., 2012) and anti-HIV or antitumor activities (Li and Wang, 2006) to treatment of hypertension and heart failure (Yoneyama et al., 2002). The efficacy of forskolin relies on activation of the adenylate cyclase enzyme (Seamon et al., 1981; Daly, 1984), leading to a marked increase of the intracellular level of cAMP (3′-5′-cAMP) in mammalian in vitro and in vivo systems (Alasbahi and Melzig, 2010b). The semisynthetic forskolin derivative NKH477 has been approved for commercial use in Japan for treatment of cardiac surgery complications, heart failure, and cerebral vasospasm (Toya et al., 1998; Kikura et al., 2004), while a forskolin eye drop solution

[1] This work was supported by the Investment Capital for University Research Center for Synthetic Biology "bioSYNergy" at the University of Copenhagen, the Research Initiative of the Danish Ministry of Science, Technology, and Innovation (to Br.H. and B.L.M.), the Novo Nordisk Foundation Center for Biosustainability (to Br.H. and B.L.M.), a personal postdoctoral stipend awarded by the FP7 PEOPLE MARIE CURIE ACTIONS Intra-European Fellowships, the PhytoMetaSyn Project (funds to J.B.) funded by Genome Canada, Genome Alberta, Government of Alberta, Genome British Columbia, Genome Prairie, Genome Quebec, National Research Council of Canada, Canada Foundation for Innovation, Ontario Ministry of Research and Innovation, McGill Innovation Centre, and the Ministère du Développement Économique, Innovation et Exportation, the Villum Foundation and the research center "Plant Plasticity" (to B.L.M.), the Danish Council on Technology and Production Sciences (to B.L.M.), and the Natural Sciences and Engineering Research Council of Canada (funds to J.B.).

[2] These authors contributed equally to the article.

* Address correspondence to bjoernh@life.ku.dk.

The author responsible for distribution of materials integral to the findings presented in this article in accordance with the policy described in the Instructions for Authors (www.plantphysiol.org) is: Björn Hamberger (bjoernh@life.ku.dk).

[W] The online version of this article contains Web-only data.

[OPEN] Articles can be viewed online without a subscription.

www.plantphysiol.org/cgi/doi/10.1104/pp.113.228429

was recently approved as an effective treatment for glaucoma (Wagh et al., 2012). Despite much effort, the full stereospecific synthesis of forskolin has not yet been achieved with current methods yielding racemic mixtures (Ye et al., 2009).

The chemical complexity of *C. forskohlii* has been well studied, and a total of 68 different diterpenoids have been isolated and identified from different tissues of the plant, of which 25 belong to the class of abietanes and 43 to the class of labdanes (Alasbahi and Melzig, 2010a). While the tricyclic abietane diterpenes have been reported to accumulate predominantly in the aerial parts, labdane diterpenoids with a bicyclic decalin core were detected primarily in the roots. Forskolin is a representative of an unusual series of tricyclic (8,13)-epoxy-labdanes, characteristic for this plant. Given its importance as a pharmaceutical, we set out to discover genes involved in the biosynthesis of forskolin. Our general approach utilized and built on a recently established diterpene pathway gene discovery strategy in nonmodel systems (Zerbe et al., 2013). As guiding principles, we considered possible spatial separation of different diterpenoid pathways in *C. forskohlii*, the large diversity of diterpenoids found in *C. forskohlii*, and the particular heterocyclic structure of forskolin. Based on the identification of putative labdane intermediates en route to forskolin in hairy root cultures of *C. forskohlii*, a pathway from trans-geranylgeranyl diphosphate (GGPP) to forskolin has recently been hypothesized (Asada et al., 2012).

GGPP is synthesized in plant plastids by the plastidial methylerythritol 4-P pathway (Rodríguez-Concepción and Boronat, 2002). For the formation of labdane-type diterpenoids in angiosperms, GGPP undergoes an initial protonation-initiated cationic cycloisomerization to a labdadienyl/copalyl diphosphate intermediate, catalyzed by class II diterpene synthase (diTPS) enzymes (Peters, 2010; Chen et al., 2011). The class II diTPS reaction, which forms the bicyclic decalin core of labdane-type diterpenoids, is terminated either by deprotonation or by water capture of the diphosphate carbocation. Subsequently, class I diTPSs catalyze cleavage of the diphosphate group and often additional cyclization or rearrangement reactions on the resulting carbocation. As with the class II diTPSs, deprotonation or water capture terminate the class I diTPS reaction. Water capture as a mechanism of diTPSs that leads to oxygen functionalities in the diterpene products has been described for the class II active site of bifunctional class I/II gymnosperm diTPSs (Keeling et al., 2011; Zerbe et al., 2012, 2013), class II angiosperm diTPSs (Falara et al., 2010; Caniard et al., 2012; Zerbe et al., 2013), and class I angiosperm diTPS (Caniard et al., 2012). Further oxidative functionalization of diterpenoids is typically catalyzed by cytochrome P450-dependent monooxygenase enzymes (P450s; Ro et al., 2005; Swaminathan et al., 2009; Hamberger et al., 2011; Wang et al., 2011; Guo et al., 2013; Hamberger and Bak, 2013), which then provide molecular handles for addition of auxiliary functional groups, leading ultimately to highly complex and decorated products such as forskolin and its derivatives.

Recently, Zerbe et al. (2013) reported the sequencing and assembly of a root transcriptome of *C. forskohlii* using 454 and Illumina sequencing technologies. Mining of the transcriptome databases resulted in the identification of a panel of candidate *CfTPS* genes. Here, we describe the functional characterization of five of them. Specifically, we demonstrate the function of CfTPS2 in combination with CfTPS3 in the stereospecific biosynthesis of (13R) manoyl oxide, the putative precursor of forskolin. We show that forskolin accumulates within a specific cell type of the root, the cork cells. Oil body-like structures characteristic and unique for this type of cell are found in the cytosol. We propose that these oil body-like structures facilitate the accumulation of high amounts of lipophilic diterpene metabolites.

RESULTS

Identification of Unique Lipophilic Organelles in *C. forskohlii* Root Cork Cells

Although high-level accumulation of forskolin-related labdanes in the root of *C. forskohlii* is well established, the localization of the biosynthetic pathway and specialized anatomical structures for the storage of diterpenes have not been reported. When transverse sections of *C. forskohlii* root (Fig. 1A) were examined using light microscopy, we found that cells of the root cork contained oil body-like structures (hereafter termed oil bodies) with a typical distribution of one oil body per cell of the root cork (Fig. 1B). These oil bodies appeared to be highly characteristic of the cork tissue, because they were not found in other cell types of the root. In sections of younger parts of the root, the oil bodies appeared yellow and occurred as single compartments within the cytoplasm of the immature cork cells (Fig. 1B). The color and pigmentation of oil bodies was observed to change with tissue maturation, possibly indicating developmental changes in their metabolite profile (Fig. 1B). In addition, cells containing more than one oil body were occasionally seen in older tissue (Fig. 1C). Further microscopy of other tissues revealed only sporadic occurrence of oil bodies in stem cork tissue (Supplemental Fig. S1).

To probe the nature of the oil bodies, histochemical staining was performed with Nile Red (9-diethylamino-5H-benzo-[α]-phenoxazine-5-one). Nile Red is a selective lipid-specific dye that is strongly fluorescent only in a hydrophobic environment. Its emission spectrum shifts depending on the polarity of its microenvironment, fluorescing magenta in the presence of polar lipids and green in the presence of neutral lipids (Diaz et al., 2008). Confocal laser scanning microscopy of *C. forskohlii* root cork stained with Nile Red indicated that the observed structures were oil bodies and that the composition of the lipophilic content was heterogeneous. Both neutral

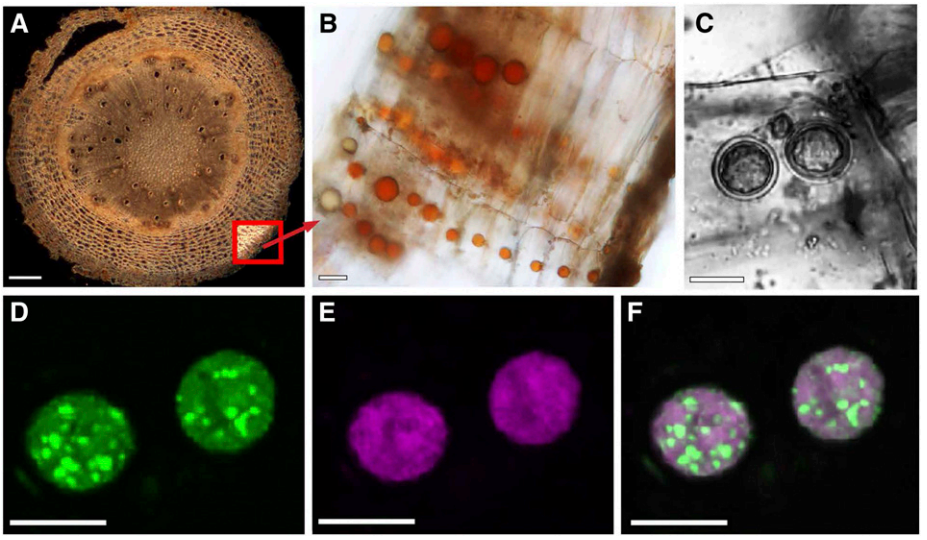

Figure 1. Localization of oil bodies within the root cork of *C. forskohlii*. A, Cross section of entire root with thick-fissured cork. Bottom right inset, the location of cork cells. B, Rows of cork cells each with one prominent oil body. C to F, Confocal imaging of Nile Red-labeled oil bodies. C, Transmitted light image of a cork cell with two oil bodies. Fluorescence images of the same oil bodies showing discrimination between neutral lipids (green fluorescence, D) and polar lipids (magenta fluorescence, E). F, Overlay of the two fluorescence images. Bars = 200 μm (A) and 10 μm (B–F).

(Fig. 1D) and polar (Fig. 1E) lipophilic compounds were observed to be nonuniformly distributed in the oil bodies with globules of neutral lipids dispersed in a predominantly polar lipid matrix (Fig. 1, D–F).

Localization of Forskolin and (13R) Manoyl Oxide in Root Cork Oil Bodies

As a first step to test whether the occurrence of forskolin is associated with the presence of oil bodies, we confirmed the localization of forskolin in the root cork. Separate methanol extracts of the root cork and the root cortex and stele were analyzed by HPLC using an evaporative light scattering detector (ELSD) and compared with flowers, leaves, and stems. Forskolin was primarily detected in the root cork and was not found in the root cortex and stele, leaves, or flowers (Fig. 2). Traces of forskolin were detected in the stem, consistent with the observed sporadic presence of a small number of oil bodies in stem cork tissue (Supplemental Fig. S1). To further examine if forskolin was present specifically in the oil bodies, methanol extracts of isolated oil bodies purified to apparent homogeneity (Fig. 3C) were subjected to HPLC-mass spectrometry (MS). Forskolin was detected in these structures, along with ions matching forskolin-related compounds (Fig. 3A; Table I). Ion peaks consistent with abietane-type diterpenes previously reported from *C. forskohlii* were also present in oil bodies (Table I).

To search for diterpenoid backbones that could serve as precursors to forskolin or to different abietane diterpenoids, isolated oil bodies as well as root cork, root cortex and stele, stem, leaves, and flowers were extracted with hexane, and the resulting extracts were analyzed by gas chromatography (GC)-MS (Figs. 3 and 4). (13R) Manoyl oxide was detected in root cork and, more specifically, in oil bodies isolated from this tissue (Fig. 3C), as well as in the root cortex and stele, stem, and flowers (Figs. 3, B and E, and 4). The localization of this compound to oil bodies is noteworthy given that it is considered the simplest diterpenoid backbone structure of forskolin and contains the correct stereochemical configuration (Fig. 3D). The abietane-type diterpenes miltiradiene, abietadiene, and dehydroabietadiene were also detected in various tissues (Fig. 4). Dehydroabietadiene was predominantly found in both types of root tissue, while abietadiene was mainly detected in the root cork tissue and miltiradiene in the stem and leaf tissue of *C. forskohlii* (Fig. 4).

C. forskohlii diTPSs Constitute a Small Gene Family

To investigate the molecular underpinnings of the diversity of diterpenoids found in the roots of *C. forskohlii*, we mined the root transcriptome of *C. forskohlii* for the

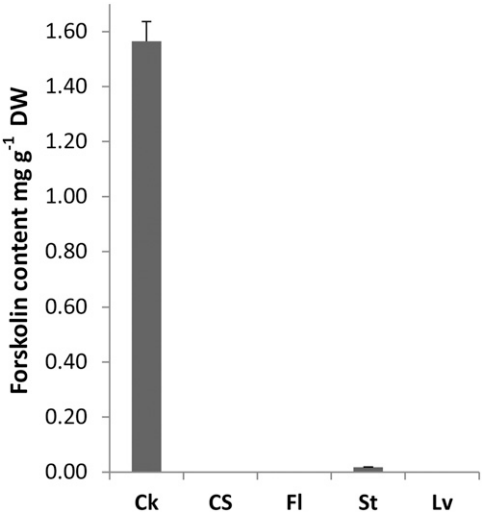

Figure 2. Forskolin content (mg g^{-1} dry weight [DW]) as determined by HPLC-ELSD analysis from different tissues of *C. forskohlii*. Data are the mean ± SE of three independent biological replicates. Ck, Root cork; CS, root cortex and stele; Fl, flowers; St, stems; Lv, leaves.

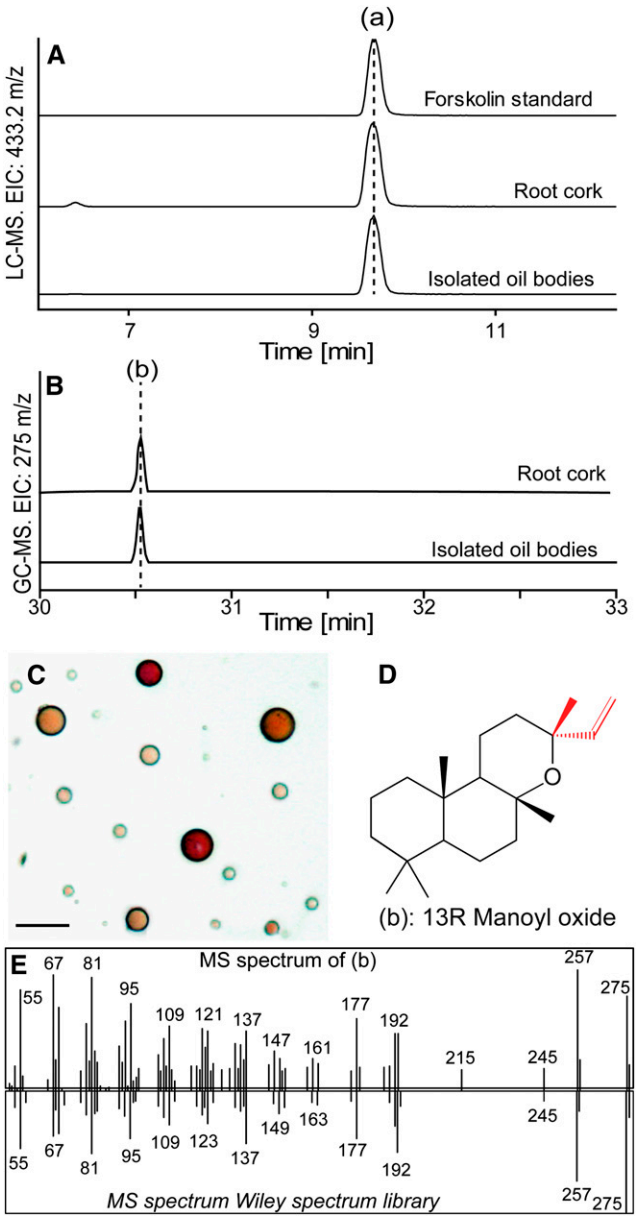

Figure 3. Detection of forskolin (a) and (13R) manoyl oxide (b) in *C. forskohlii* root cork and isolated oil bodies. A, LC-MS EIC of *m/z* 433.2197 $[\text{forskolin} + \text{Na}]^+$ in isolated oil bodies and in root cork tissue from *C. forskohlii*. B, GC-MS EIC of *m/z* 275 corresponding to manoyl oxide in isolated oil bodies and in root cork tissue from *C. forskohlii*. C, Bright-field microscope image of isolated *C. forskohlii* oil bodies. Bar = 5 μm. D, Molecular structure of (13R) manoyl oxide. E, Mass spectrum obtained from manoyl oxide identified in root cork tissue (top) and reference spectrum (bottom) from Wiley mass spectrum database.

identification of *CfTPS* candidates (Zerbe et al., 2013). A panel of six diterpene synthases was identified, *CfTPS1*, *CfTPS2*, *CfTPS3*, *CfTPS4*, *CfTPS14*, and *CfTPS15*, which, with exception of *CfTPS15*, represented full-length complementary DNAs (cDNAs) with predicted N-terminal plastidial transit peptides. *CfTPS1*, *CfTPS2*, and *CfTPS15* contained the Asp-rich conserved motif DxDD characteristic of class II diTPS, while *CfTPS3*, *CfTPS4*, and *CfTPS14* carried the DDxxD signature motif of class I diTPS (Supplemental Fig. S2). To further substantiate the classification, relationships, and evolution of the CfTPSs, we performed separate phylogenetic analyses of class II and class I CfTPSs, including functionally characterized representatives from the Lamiaceae and other angiosperm species. Included in the phylogenies were representative gymnosperm class II and class I diTPSs from white spruce (*Picea glauca*) (PgCPS and PgEKS; Keeling et al., 2010) and the bifunctional diTPS from the moss *Physcomitrella patens* (PpCPS/EKS; Hayashi et al., 2010), as it is considered an ancestral archetype of plant diTPSs (Fig. 5).

Among the class II diTPSs, two distinct clades were apparent for dicotyledon species. One clade includes the single-copy Arabidopsis (*Arabidopsis thaliana*) AtCPS involved in general metabolism of gibberellic acid formation and orthologous from other species with characterized CPS functions. Also in this clade are paralogous gene pairs from pumpkin (*Cucurbita maxima*; CmCPS1 and CmCPS2) and *Isodon eriocalyx* (IeCPS1 and IeCPS2), which resulted from gene duplications potentially allowing for neofunctionalization of diTPS in the biosynthesis of specialized metabolites (Li et al., 2012a). In the second and apparently more divergent clade, enzymes of rock rose (*Cistus cresticus*) copal-8-ol diphosphate synthase [CcCLS], tobacco (*Nicotiana tabacum*; labda-13-en-8-ol diphosphate synthase [LPPS]; NtLPPS), and two closely related Lamiaceae (clary sage [*Salvia sclarea*; SsLPPS] and *Salvia miltiorrhiza*, SmCPS1) are involved in specialized metabolism and have been shown to produce copal-8-ol diphosphate and (+)-copalyl diphosphate, respectively (Gao et al., 2009; Caniard et al., 2012). In *C. forskohlii*, we identified CfTPS15, a single-copy class II diTPSs grouping with the bona fide CPS (general metabolism), and CfTPS1 and CfTPS2, a pair of diTPSs grouping with the class II enzymes involved in specialized metabolism.

The overall topology of the class I diTPS phylogeny resembles the class II phylogeny. One clade includes the EKS of general metabolism of gibberellic acid formation together with a set of rice (*Oryza sativa*) class I diTPS that evolved through species-specific duplications associated with neofunctionalization in rice-specialized metabolism (Morrone et al., 2011). CfTPS14 falls into this clade. A separate clade contains members involved in specialized metabolism, including tobacco NtCAS, converting copal-8-ol diphosphate to the specialized metabolite cis-abienol (Sallaud et al., 2012). The enzymes from *S. sclarea* and *S. miltiorrhiza*, producing the labdane-specialized metabolites sclareol (SsSCS) and the abietane miltiradiene, respectively (Gao et al., 2009; Caniard et al., 2012), are members of a subgroup consisting of Lamiaceae enzymes. A second pair of *C. forskohlii* diTPS, CfTPS3 and CfTPS4, is clustered with this clade. All members of this group of Lamiaceae sequences represent bidomain ($\beta\alpha$) class I diTPS, lacking the γ-domain.

Table I. *Abietane- and labdane-type diterpenoids detected by LC-MS analysis of oil bodies isolated from C. forskohlii root cork*

Compounds were identified based on accurate mass measurements with the exception of forskolin, which was also identified based on coelution with an authentic standard.

Retention time	*m/z*	Adduct	Predicted Formula	Mass Accuracy	Compound	Reference
min				*mg L*$^{-1}$		
6.69	331.1901	$[M + H]^+$	$C_{20}H_{26}O_4$	0.87	14-deoxycoleon U	Xu et al., 2005
9.64	375.2159	$[M + Na]^+$	$C_{20}H_{32}O_5$	−4.84	Deoxy-deacetyl-forskolin	Asada et al., 2012
9.67	433.2194	$[M + Na]^+$	$C_{22}H_{34}O_7$	0.67	Forskolin	Bhat et al., 1977
10.88	401.2298	$[M + Na]^+$	$C_{22}H_{34}O_5$	0.12	Dideoxy-forskolin	Asada et al., 2012
14.20	317.2102	$[M + H]^+$	$C_{20}H_{28}O_3$	2.91	20-Deoxocarnosol	Kelecom, 1984
16.11	417.2252	$[M + Na]^+$	$C_{22}H_{34}O_6$	−1.12	Deoxy-forskolin	Asada et al., 2012
18.29	385.2341	$[M + Na]^+$	$C_{22}H_{34}O_4$	2.16	Trideoxy-forskolin	Asada et al., 2012
22.95	323.1967	$[M + Na]^+$	$C_{20}H_{28}O_2$	4.83	Barbatusol	Kelecom, 1983

Transcript Levels of *C. forskohlii* diTPSs in Various Tissues

To correlate the transcript levels of *CfTPS* genes with accumulation of forskolin-related labdane diterpenoids and abietane diterpenoids in *C. forskohlii* tissues, quantitative reverse transcription-PCR analysis was performed using cDNA templates derived from total RNA extracted from root cork, root cortex and stele (root without cork), leaves, stems, and flowers. *CfTPS1*, *CfTPS2*, and *CfTPS3* shared similar transcript profiles patterns across all tissues, with high transcript accumulation in root cork cells, up to 1,000-fold compared with all other tissues tested (Fig. 6). These data provide support for the involvement of *CfTPS1*, *CfTPS2*, and *CfTPS3* in the formation of specialized metabolites in the root cork. By contrast, the transcript levels of *CfTPS4*, *CfTPS14*, and *CfTPS15* were relatively low across all tissues tested. Despite the close phylogenetic relation of *CfTPS3* and *CfTPS4* (Fig. 5), they show surprisingly different expression patterns. In contrast to *CfTPS3*, *CfTPS4* transcripts were mostly detected in the aerial parts of the plant, especially in the leaves, while its transcripts accumulate only to very low levels in the root (Fig. 6).

Transcript profiles of the individual *CfTPS* genes, including both spatial patterns of distribution across tissues and relative transcript abundance, support a role for *CfTPS14* and *CfTPS15* in general metabolism and the involvement of *CfTPS1*, *CfTPS2*, and *CfTPS3* in localized, active biosynthesis of specialized metabolites. These patterns are also in agreement with the results of the phylogenetic analysis (Fig. 5). Transcript profiles did not provide indications for a role of *CfTPS4*.

In Vitro Functional Characterization of *C. forskohlii* diTPSs

For the functional characterization of the CfTPSs described here (except for CfTPS15, for which no full-length sequence could be retrieved), cDNAs were heterologously expressed in *Escherichia coli* with a C-terminal 6×His epitope tag. Purified recombinant proteins were tested individually in single or coupled in vitro assays and supplied with appropriate substrates, and the reaction products were analyzed by GC-MS. Products of the in vitro single assays with the class II diTSPs, CfTPS1 and CfTPS2, were treated with alkaline phosphatase before GC-MS analysis.

Enzyme assays with CfTPS1 yielded a diterpene with a mass spectrum matching copal-15-ol, indicating that the primary product before dephosphorylation is copalyl diphosphate (Fig. 7A). Assays of CfTPS2 resulted in the formation of 13(16)-14-labdien-8-ol and labd-13-en-8,15-diol as major products (Fig. 7B), supporting a function as labda-13-en-8-ol (or copal-8-ol) diphosphate

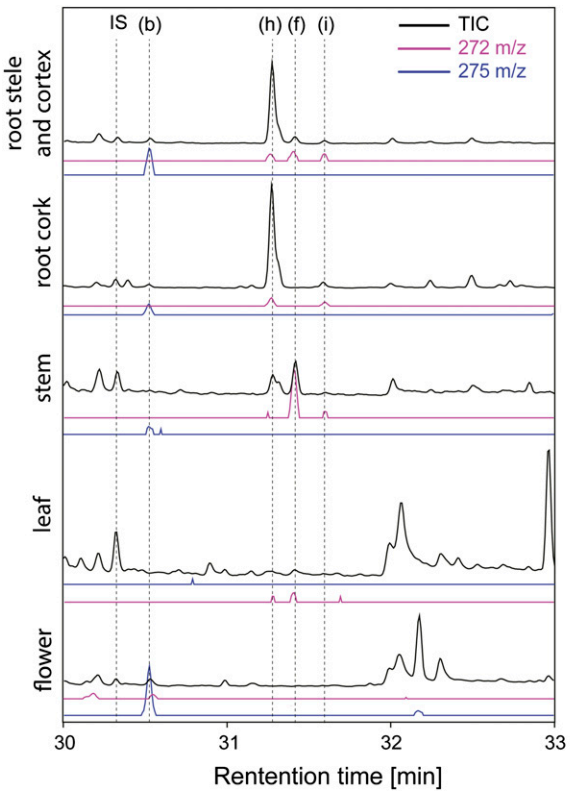

Figure 4. GC-MS analysis of hexane extracts from *C. forskohlii* tissues. The letter "b" indicates (13R) manoyl oxide, "h" indicates dehydroabietadiene, "f" indicates miltiradiene, and "i" indicates abietadiene. IS, Internal standard (1 mg L^{-1} 1-eicosene).

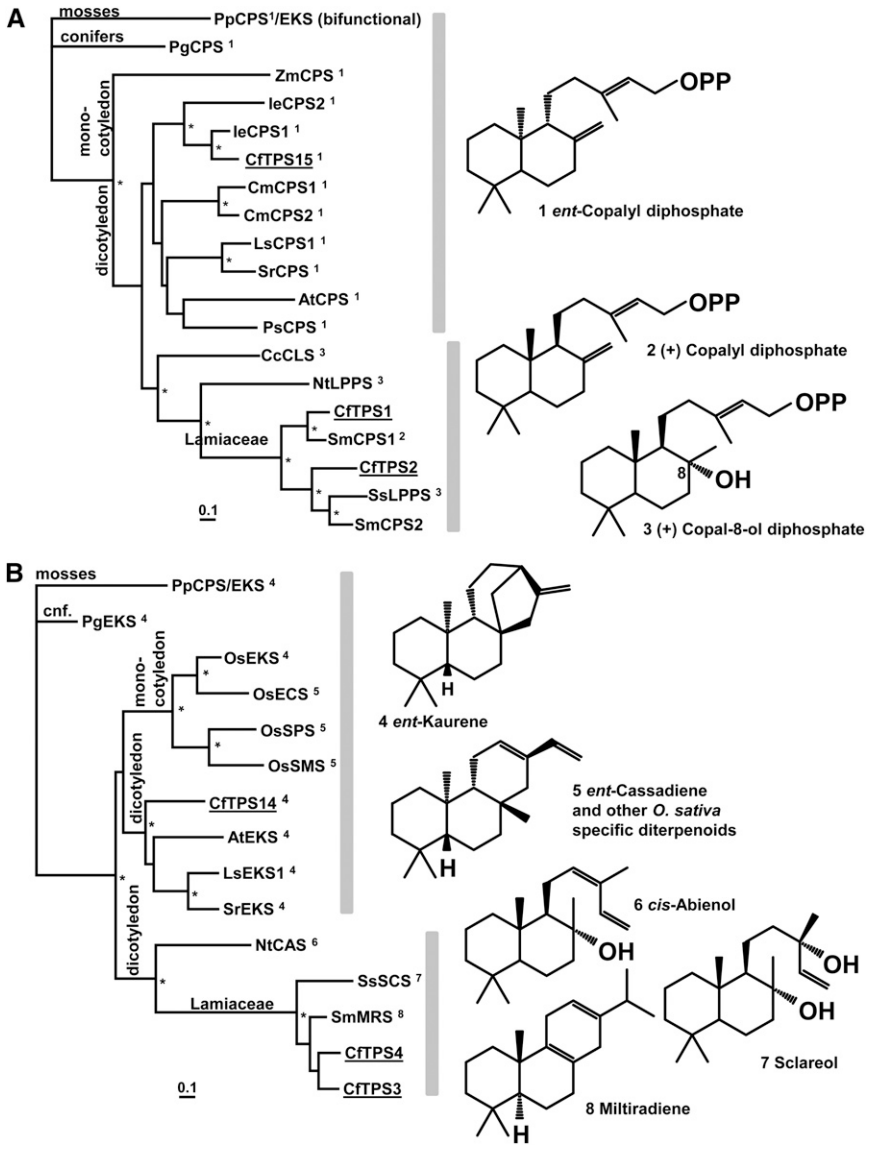

Figure 5. Phylogenetic classification of *C. forskohlii* diterpene synthases with known class II (A) and class I (B) sequences. The phylograms are rooted with the bifunctional *ent*-copalyl diphosphate synthase/*ent*-kaurene synthase from the moss *P. patens*. Asterisks indicate nodes supported by greater than 80% bootstrap confidence, and the scale bar indicates 0.1 amino acid changes. The numbers indicated at each enzyme refer to their respective enzymatic products, the structures of which are given on the right. Species and GenBank accession are given in Supplemental Table S2.

synthase, similar to the functions of previously reported similar enzymes (Falara et al., 2010; Caniard et al., 2012; Sallaud et al., 2012; Zerbe et al., 2013). We also detected the nonstereoselective formation of the (13R) and (13S) epimers of manoyl oxide, which were previously observed in in vitro reactions of similar class II diTPSs and were suggested to be the result of a nonenzymatic reaction (Caniard et al., 2012; Zerbe et al., 2013). These results indicate that CfTPS1 and CfTPS2 represent functionally distinct class II diTPSs, both necessary and sufficient to form the diphosphate intermediates required for the abietane and labdane classes of diterpenoids detected in the root of *C. forskohlii*.

The overall expression level of CfTPS14 in *E. coli* cells was low, with little activity in coupled assays with CfTPS1 and no detectable product formation in combination with CfTPS2 (data not shown). However, we have previously suggested a function based on coexpression with a diTPS from *Euphorbia peplus* (Zerbe et al., 2013), which supports a function of CfTPS14 in the general metabolism of gibberellin phytohormones. Assays of CfTPS1 coupled to either CfTPS3 or CfTPS4 resulted in formation of miltiradiene (Fig. 7A), an abietane diterpene formed from a copalyl diphosphate intermediate (Gao et al., 2009), and is consistent with the results of the single enzyme assay of CfTPS1. Coupled assays with CfTPS2 and CfTPS3 showed the formation of the pure (13R) enantiomer of manoyl oxide (Fig. 7B), supporting a role of CfTPS2 in formation of the copal-8-ol diphosphate intermediate as detected in the single enzyme assay. In coupled assays of CfTPS2 with CfTPS4, both (13R) and (13S) manoyl oxide epimers were detected, albeit at a ratio different from the dephosphorylation product of CfTPS2 alone (Fig. 7B). The stereospecific production of the (13R) manoyl oxide epimer when CfTPS2 (class II)

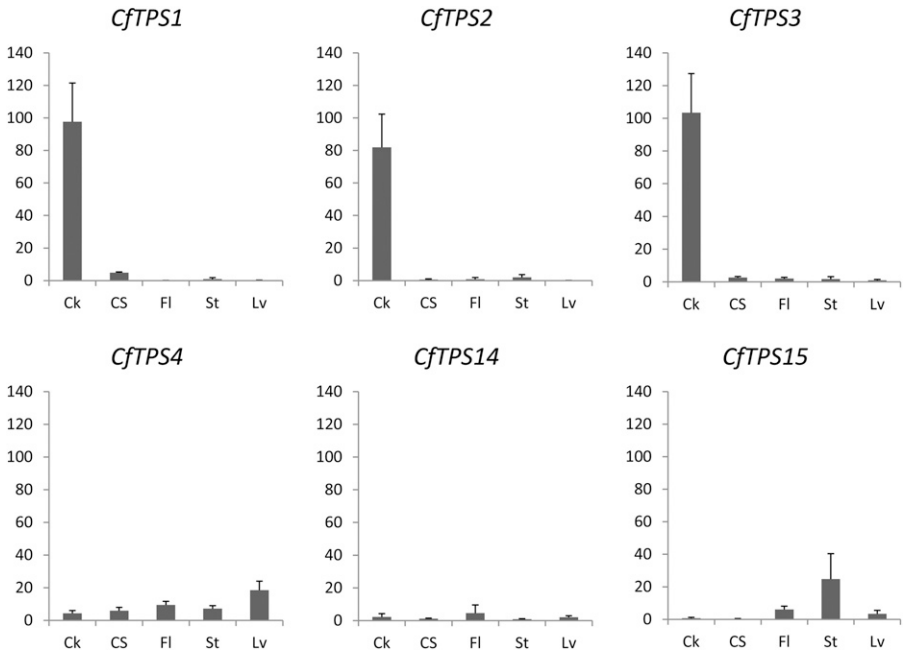

Figure 6. Relative expression of *CfTPS* genes in *C. forskohlii* tissues. Transcript abundance of *CfTPS* genes expressed in arbitrary units was measured by quantitative PCR using the translation initiation factor (TIF4a) for normalization. Each value represents the average of three biological replicates, each of which was performed in at least three technical replicates. Ck, Root cork; CS, root cortex and stele; Fl, flowers; St, stems; Lv, leaves.

and CfTPS3 (class I) enzymes were combined, along with their transcriptional coexpression in root cork tissue, where (13R) manoyl oxide and forskolin were detected, supports their involvement in the formation of the intermediate of forskolin in planta. Single enzyme assays using CfTPS3 and CfTPS4 with geranyl diphosphate (GPP) as substrate did not result in any product formation (Supplemental Fig. S3).

In Planta Heterologous Expression and Functional Characterization of *C. forskohlii* diTPSs

To validate the results obtained with CfTPS produced as recombinant proteins in *E. coli*, we investigated the in planta function of the CfTPSs by transient heterologous expression in *Nicotiana benthamiana* leaves after agroinfiltration. GC-MS analyses of extracts from *N. benthamiana* leaves transiently expressing the individual class I CfTPS3, CfTPS4, and CfTPS14 did not result in detectable accumulation of additional metabolites compared with control plants (data not shown). Extracts from *N. benthamiana* expressing the class II CfTPS1 alone showed only trace amounts of additional diterpenes compared with the controls, none of which could be accurately identified (Fig. 8B). Consistent with the in vitro enzyme assays, both (13R) and (13S) epimers of manoyl oxide were identified in the extracts from *N. benthamiana* expressing the class II CfTPS2 (Fig. 8A). Coexpression of CfTPS2 and CfTPS14 did not change the product profile compared with expression of CfTPS2 alone, suggesting that CfTPS14 does not accept the copal-8-ol diphosphate as substrate (Fig. 8A). In extracts of plants coexpressing CfTPS1 with CfTPS3 or CfTPS4, miltiradiene was observed as the main product together with minor traces of dehydroabietadiene and abietadiene (Fig. 8B).

In extracts from *N. benthamiana* coexpressing CfTPS2 with CfTPS3 or CfTPS4, only the (13R) epimer of manoyl oxide was identified (Fig. 8A), consistent with the stereochemical conformation of forskolin and the related series of labdane-type diterpenoids. This result suggests that the class I CfTPS3 and CfTPS4 can accept the copal-8-ol diphosphate synthesized by CfTPS2 and catalyze the stereospecific formation of (13R) manoyl oxide.

DISCUSSION

Intracellular Accumulation of Diterpenes in the *C. forskohlii* Root Cork May Be Facilitated by Unique Hydrophobic Oil Body Structures: A Suitable Means for Near-Surface Sequestration of Terpenoids in Roots

Plants have evolved both specialized mechanisms and specialized anatomical structures for the secretion, sequestration, and accumulation of defense-related and potentially toxic molecules (Morant et al., 2008; Schilmiller et al., 2008; Sirikantaramas et al., 2008). These metabolites may otherwise display adverse activities for the producing plant cell. Intracellular storage of such biologically active metabolites in the vacuole is well established for water-soluble compounds and for compounds that become water soluble through conjugation (Marinova et al., 2007; Ferreres et al., 2011; Zhao et al., 2011; Li et al., 2012b). Similarly, for the large class of often-lipophilic terpenoids, it has been suggested that their intracellular accumulation may be limited by nonspecific interference with cellular

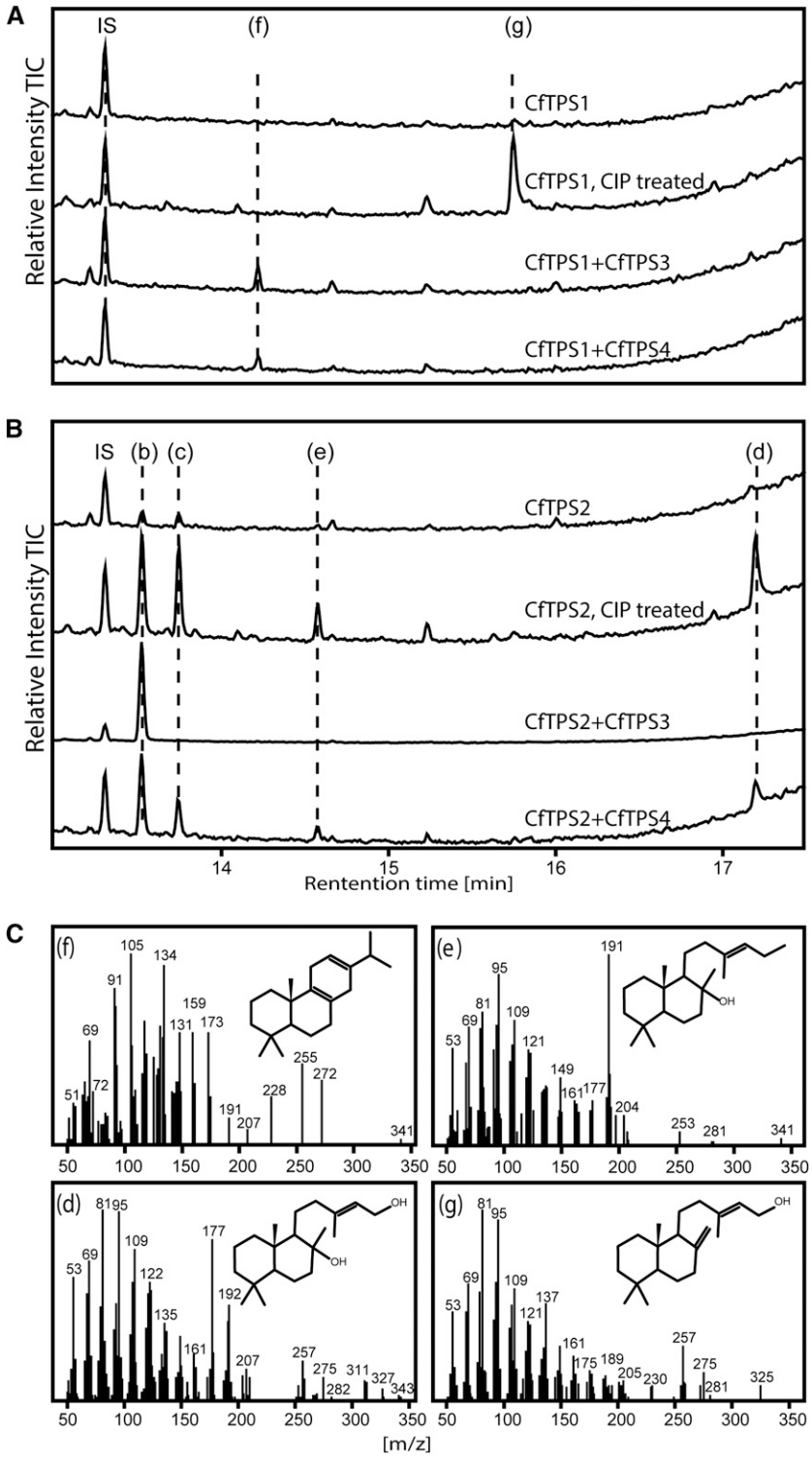

Figure 7. GC-MS analysis of in vitro assays with *C. forskohlii* diTPS. A, In vitro assays with CfTPS1 alone and coupled assays with CfTPS1 and CfTPS3 and CfTPS4. Extracts of CfTPS1 assays were treated with calf intestinal alkaline phosphatase (CIP). B, In vitro assays with CfTPS2 and coupled with CfTPS3 and CfTPS4. Extracts of CfTPS2 were treated with calf intestinal alkaline phosphatase. The letter "b" indicates (13R) manoyl oxide, "c" indicates (13S) manoyl oxide, "d" indicates labd-13-en-8,15-diol, "e" indicates labden-8-ol, "f" indicates miltiradiene, and "g" indicates copal-15-ol. IS, Internal standard (1 mg L^{-1} 1-eicosene). C, Mass spectra of compounds identified from assays. Structures tentatively identified as described in "Materials and Methods."

processes and structures, such as interaction with membrane integrity (Uribe et al., 1985; Gershenzon and Dudareva, 2007; Sirikantaramas et al., 2008; Zore et al., 2011). Plant anatomical features and cellular structures typically associated with the biosynthesis and storage of large amounts of terpenoids are well studied and include glandular trichomes (Gershenzon et al., 2000; Iijima et al., 2004; Siebert, 2004; Schilmiller et al., 2008; Xie et al., 2008; Chatzopoulou et al., 2010; Lane et al., 2010), laticifer cells (Mahlberg, 1993; Post et al., 2012), resin cells, resin blisters, or resin ducts (Martin et al., 2002; Zulak and Bohlmann, 2010), and glandular cavities lined by epithelial cells (Heskes et al., 2012; Voo et al., 2012).

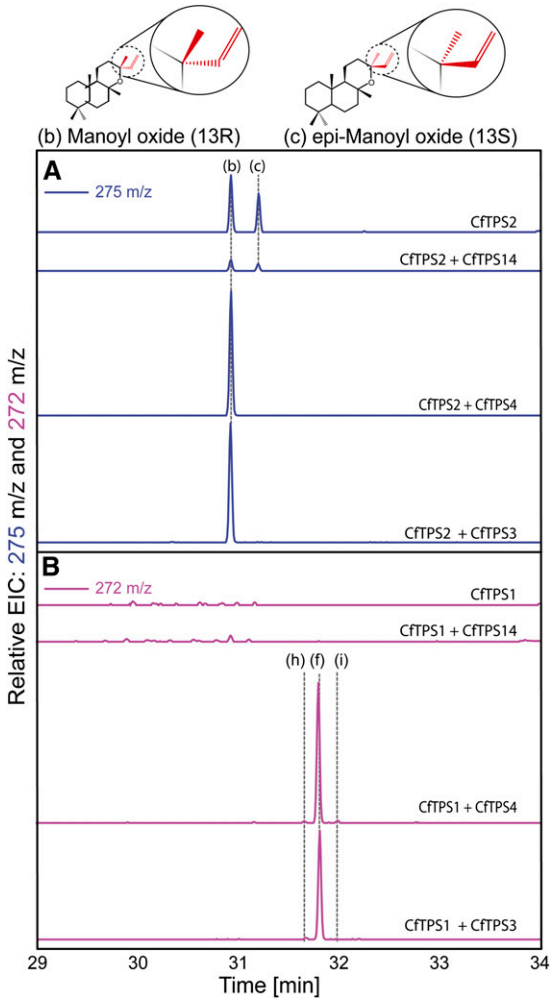

Figure 8. GC-MS analysis of hexane extracts from *N. benthamiana* transiently expressing *C. forskohlii* diTPSs. A, EIC of *m/z* 275. B, EIC of *m/z* 272. The letter "b" indicates (13R) manoyl oxide, "c" indicates (13S) manoyl oxide, "h" indicates dehydroabietadiene, "f" indicates miltiradiene, and "i" indicates trace amount of abietadiene.

Here, we showed accumulation of the partly lipophilic diterpenoid forskolin and the presence of its precursor, (13R) manoyl oxide, together with a series of other labdane- and abietane-type diterpenoids, in root cork cells of *C. forskohlii*. In these unique cell types, large oil bodies represent dominant and highly characteristic intracellular compartments that are not found in other tissues of the plant. Interestingly, the presence of both forskolin and (13R) manoyl oxide in these oil bodies indicates that the biosynthetic route to forskolin is active in this specific cell type. Accumulation of forskolin specifically in these oil bodies may facilitate the effective storage of terpenoids in a localized intracellular and lipophilic environment that is compartmentalized from the rest of the cytosol. Our designation of these oil bodies as terpenoid accumulation compartments in the cork cells of *C. forskohlii* roots extends the known anatomical repertoire of specialized cells and cell compartments for producing and accumulating biologically active terpenoids in plants.

Given the biological activities of diterpenoids such as forskolin and their high level of accumulation in oil bodies of root cork cells, the diterpenoid-enriched root cork could provide a barrier against soil-born pests or pathogens. For the roots of *C. forskohlii*, the near-to-the-surface sequestration of terpenoids in a cork layer may serve a similar protective function below ground, as is attributed to glandular trichomes on surfaces of the above-ground parts of plants. Glandular trichomes exist on the above-ground parts of *C. forskohlii* but are generally not known to exist on root surfaces. The exclusive accumulation of forskolin, and detection of manoyl oxide and a series of related labdane diterpenoids in the cells of the root cork and the fact that labdane-type diterpenoids have been implied before in plant defense against microbes (Fragoso-Serrano et al., 1999; Habibi et al., 2000; Peters, 2006; da Silva et al., 2008), suggests a specific role of these compounds in the interaction of the plant root with the soil ecosystem and defense.

A New Role for Oil Bodies

Oil bodies are intracellular organelles mainly consisting of neutral lipids such as triacylglycerides, which have been suggested to function as carbon and energy reserves activated under starvation or rapid growth conditions (Penno et al., 2013). In some plant species oil bodies have also been associated with stress responses, hormone signaling, plant growth and development, and sterol biosynthesis (Fujimoto and Parton, 2011; Chapman et al., 2012; Silvestro et al., 2013). In liverworts (of the plant division *Marchantiophyta*), these types of organelles have been suggested to cooccur with terpenoids (He et al., 2013). In vascular plants, oil body structures have been detected in several parts of the plant including seeds, leaves, flowers, pollen, and fruits. Oil bodies are considered to be derived from the endoplasmic reticulum, resulting from the accumulation of triacylglycerides between the endoplasmic reticulum bilayer, followed by budding of the cytoplasm-oriented membrane to form the newly generated oil bodies (Beller et al., 2010; Chapman et al., 2012; Murphy, 2012). Our findings of oil bodies with a heterogeneous composition including diterpenoids and localization to the cork of the *C. forskohlii* root suggest additional functions of oil bodies in the sequestration of specialized metabolites and possibly plant defense (as discussed above).

Evolution of the *C. forskohlii* diTPS Family Toward Chemical Diversity

Screening of the *C. forskohlii* root transcriptome resulted in the identification of a small CfTPS gene family. Single-copy class I and class II diTPS candidates

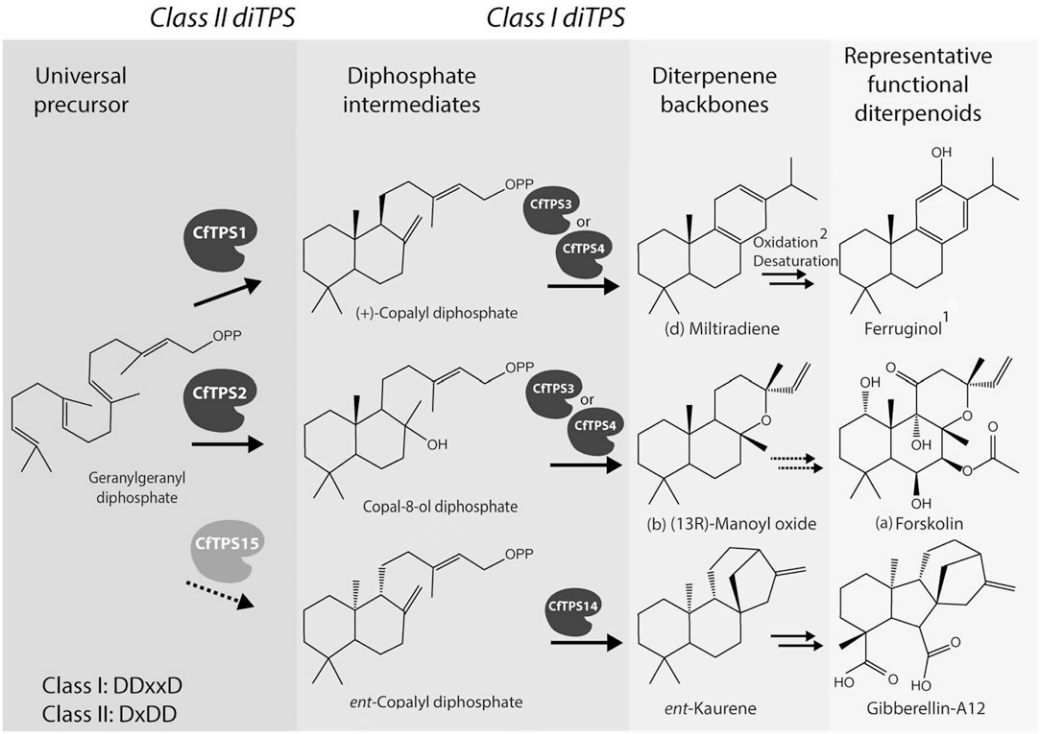

Figure 9. Scheme of the biosynthetic routes from GGPP to specialized and general diterpenoids of the abietane, labdane, and *ent*-kaurene class. Dashed arrows indicate reactions without experimental evidence in *C. forskohlii*. [1]Detection of (+)-ferruginol in *C. forskohlii* was reported earlier (Hurley, 1998); [2]CYP76AH1 from the close relative *S. miltiorrhiza* was proposed to convert miltiradiene to ferruginol (Guo et al., 2013).

likely required for general metabolism, as well as pairs of duplicated class I and class II diTPS candidates potentially involved in specialized metabolism, have been identified. Based on phylogenetic relations and transcript profiles, we hypothesized involvement of CfTPS1, CfTPS2, CfTPS3, and CfTPS4 in specialized metabolism and a role for CfTPS14 and CfTPS15 in general metabolism of gibberellin phytohormone biosynthesis. DiTPS genes of general metabolism can serve as a template for gene duplication, which, in turn, could facilitate the evolution of genes with novel functions in specialized metabolism (for review, see Chen et al., 2011). Here, we traced such events from the phylogenetic relationships of the six different CfTPSs and substantiated them with functional characterization.

Originating from a class I/II bifunctional diTPS progenitor, angiosperm and gymnosperm diTPSs are thought to have evolved in two distinct clades, the class II or CPS and CPS-derived and the class I or EKS and EKS-derived enzymes (Chen et al., 2011). Additional clades of bifunctional or monofunctional diTPSs exist outside of the angiosperms (Zerbe et al., 2013). Within the two clades of class I and class II diTPSs, several branches of angiosperm diTPSs involved in specialized metabolism indicate events of lineage-specific diversification through gene duplication and neofunctionalization. Events of neofunctionalization may be limited to recruitment of the enzyme to a novel pathway, yet retaining its original CPS or EKS enzymatic function, or may have led to novel enzymatic functions (with or without loss of the original function). Examples are class II diTPSs involved in the metabolism of specialized diterpenes, such as *I. eriocalyx IeCPS2* (Li et al., 2012a) derived from a recent duplication of *IeCPS1* and retaining *ent*-CPS activity. By contrast, *S. miltiorrhiza* SmCPS, tobacco NtLPPS, and *S. sclarea* ScSCS represent CPS-like diTPS with novel enzymatic functions (Gao et al., 2009; Caniard et al., 2012; Sallaud et al., 2012). Results from our work in *C. forskohlii* support a model of evolution through gene duplication, neofunctionalization, and loss of ancestral *ent*-CPS activity leading to CfTPS1 and CfTPS2.

For the class I clade of diTPS, separation of functionalities in general and specialized metabolism may be more challenging to assign. Enzymes of this clade may acquire the capacity to accept novel substrates while also retaining activity toward copalyl diphosphate. CfTPS14 appears to be a bona fide EKS with a likely function in gibberellin biosynthesis. Our results with both CfTPS3 and CfTPS4, when coupled with functionally distinct class II diTPS CfTPS1 or CfTPS2, indicate substrate promiscuity and possible redundancy between these two EKS-like enzymes in specialized metabolism. However, the distinct transcript profiles of *CfTPS3* and *CfTPS4* also indicated that the two enzymes may be involved in different functional contexts or pathways in *C. forskohlii*. *CfTPS4* is mainly expressed in

the aerial tissues of the plant, where forskolin does not accumulate. It cannot be excluded though that CfTPS4 is coupled in these tissues with specific type II diTPSs not identified in our study.

Taken together, results from in planta and in vitro assays show that a relatively small family of diTPS can generate an array of different diterpene core structures (Fig. 9) when individual enzymes are combined in higher level functional modules of pairs of class II and class I enzymes. The diterpene structures detected in our assays match those known to exist in *C. forskohlii* and represent the starting points for oxidative decorations in the plant.

Involvement of CfTPS2 and CfTPS3 in the Formation of (13R) Manoyl Oxide en Route to Forskolin in Root Cork Cells

We showed here that the two class I diTPS CfTPS3 and CfTPS4 can each be effectively coupled with either of the two class II enzymes, CfTPS1 and CfTPS2 (Fig. 9), highlighting the remarkable modularity of diterpene metabolism. *CfTPS1* was also found highly expressed in the same tissue as *CfTPS2* and *CfTPS3*, indicating that cork cells may have the capacity to produce a suite of both labdane- and abietane-type diterpenoids. Following recent gene duplication, resulting in the *CfTPS3* and *CfTPS4* pair, a change in the expression pattern could have resulted in novel functional modules of diTPSs in different tissues. This finding is supported by the gene expression studies together with the nontargeted metabolomic HPLC-MS and GC-MS analyses of the root cork metabolites, showing highly complex profiles with accurate masses characteristic of diterpenoids of labdane and abietane classes (Fig. 4; Table I).

Detection of both forskolin and (13R) manoyl oxide along with the accumulation of *CfTPS2* and *CfTPS3* transcripts in the specialized root cork cell type, together with the in vitro and in vivo functional characterization of CfTPS2 and CfTPS3, suggest that these two enzymes are involved in the early steps of forskolin biosynthesis via (13R) manoyl oxide in the root of *C. forskohlii* (Fig. 9). Transcript profiles of *CfTPS4* would make a similar conclusion for this diTPS less obvious. Racemic mixtures of (13R) and (13S) manoyl oxide have previously been reported as artifacts or side products of enzyme assays (Caniard et al., 2012; Zerbe et al., 2013), a result also described here in our in vitro assay with CfTPS2 and CfTPS4. However, the stereospecific cyclization of GGPP into the (13R) epimer of manoyl oxide by the functional module of CfTPS2 coupled with either CfTPS3 (or CfTPS4) in vivo in the *N. benthamiana* expression system is consistent with the stereochemical conformation of forskolin and the series of forskolin-related labdanes detected in *C. forskohlii* (Asada et al., 2012), as well as with the absence of the (13S) epimer of manoyl oxide in the plant tissues analyzed (Fig. 4).

While the significance of (13R) manoyl oxide is attributed to its role as a forskolin precursor, manoyl oxide itself exhibits a number of important properties, such as antibacterial or antiinflammatory activities or as a potent anticancer agent (de las Heras and Hoult, 1994; Demetzos et al., 1994; Dimas et al., 1999; Angelopoulou et al., 2001).

Functions for CfTPS1 and CfTPS3 or CfTPS4 in the Formation of Miltiradiene

Assays with modules of CfTPS1 coupled to either the CfTPS3 or CfTPS4 resulted both in vitro and in vivo in the formation of miltiradiene, an intermediate in the biosynthesis of tanshinones in the closely related *S. miltiorrhiza* (Gao et al., 2009). While miltiradiene readily rearranged to dehydroabietadiene in our experimental setup, the in planta route to the aromatic dehydroabietadiene-derived diterpenoids, which are the second dominant type in *C. forskohlii* (Alasbahi and Melzig, 2010a), remains unclear. Recently, enzymatic conversion of miltiradiene to ferruginol, a 10-hydroxy-dehydroabietadiene, by a member of the CYP76 family was reported from *S. miltiorrhiza* (Guo et al., 2013). The identification of cytochrome P450s involved in the oxidative decoration of (13R) manoyl oxide en route to forskolin and related labdane diterpenoids is now underway using existing *C. forskohlii* P450 candidate resources and through development of new transcriptome and proteome resources for the specialized cell type of the *C. forskohlii* root cork cells.

CONCLUSION

Here, we reported the functional characterization of a panel of class I and II diTPSs, including a specific pair of diTPS involved in the biosynthesis of (13R) manoyl oxide in *C. forskohlii*. Manoyl oxide, itself an anticancer compound, is a structurally unusual diterpenoid carrying an oxygen- containing heterocycle and represents the molecular core for a large series of bioactive derivatives including the cAMP modulator, forskolin. We have shown that both manoyl oxide and forskolin accumulate together in a specific root cork cell type in *C. forskohlii*, indicating a role of these cells in protective plant-environment interactions in the rhizosphere. Biosynthesis and accumulation of specialized diterpenoids in these cells may be supported by the presence of oil bodies, providing the equivalent of a compartment specialized for storage of hydrophobic bioactive metabolites. Our discovery of *C. forskohlii* diTPSs participating in the early steps of forskolin biosynthesis, as well as the involvement of oil bodies in the storage of diterpenoids, may have implications for the discovery of other biosynthetic pathways of terpenoids in nonmodel plants and in biotechnological applications aiming at the production of high-value terpenoid-based pharmaceuticals, flavors, fragrances, and other terpenoid bioproducts.

MATERIAS AND METHODS

Plant Growth and Microscopy

Coleus forskohlii (Lamiaceae) plants were grown in the greenhouse at the University of Copenhagen, Denmark under ambient photoperiod and 24°C day/17°C night temperatures. Transverse sections of roots (diameter of approximately 1–5 mm) were prepared for histochemical analysis. Sections were performed by hand or by vibrating blade microtome (100 μm; Microm HM 650 V) and observed unstained with a Leica DM 5000B or a Nikon Eclipse 80i light and fluorescence microscope.

Additionally, root samples were fixed in a solution containing 2.5% (v/v) glutaraldehyde, 2% (v/v) paraformaldehyde, and 0.1 M sodium cacodylate buffer, pH 7.2, for 24 h; thereafter, surface sections and cross sections from the root cork were incubated in 0.1 μg mL^{-1} Nile Red for identification of lipid components (Eltgroth et al., 2005). Images from intact cells were recorded on a Leica SP5X confocal laser scanning microscope. A 20× water immersion objective was used for all images. Nile Red was excited with the 514-nm line from the argon laser, and the emitted light was collected at 525 to 567 nm and at 648 to 698 nm, respectively. Autofluorescence was tested without dye using the same microscope settings. Contrast adjustments were carried out to improve clarity of images but did not alter overall appearance. Final image processing, cropping, and mounting of the images were done with Adobe Photoshop CS2 and Illustrator CS2.

Diterpene Profiling and Forskolin Quantification in *C. forskohlii* Tissues

Tissue was extracted as described in De Vos et al. (2007). Cold methanol acidified with formic acid (0.125% [v/v]) was added to ground and frozen tissue samples in a ratio of 3:1 (solvent:tissue). Samples were sonicated in an ultrasonic bath at 23°C for 15 min at 40 kHz (Branson, 3510), filtered using 96-well filter plates, and analyzed by HPLC equipped with an ELSD. All tissue types were extracted in triplicate. The HPLC-ELSD system was comprised of a Shimadzu LC-20AT pump, SIL-20A HT autosampler, and ELSD-LTII detector. Samples were separated on a Synergi 2.5 μm Fusion-RP C18 Column (50 × 2 mm; Phenomenex) at a flow rate of 0.2 mL min^{-1} with column temperature held at 25°C. The mobile phase consisted of water with 0.1% formic acid (v/v; solvent A) and acetonitrile with 0.1% formic acid (v/v; solvent B). The gradient program was 20% to 100% B over 35 min and 100% B for 1 min, followed by a return to starting conditions over 0.25 min, which was then held for 15 min to allow the column to reequilibrate. The ELSD drift tube temperature was held at 50°C, and the nitrogen drying gas pressure was 3.8 bar. Forskolin was quantified by comparison to a standard series of forskolin (Sigma).

For the diterpene profiling of isolated oil bodies, extracts were lyophilized and then dissolved in methanol and analyzed by HPLC-electrospray ionisation-high resolution mass spectrometry. Separation was carried out on an Agilent 1100 Series HPLC unit with column and gradient as described above. The liquid chromatography (LC) unit was coupled to a Bruker microTOF mass spectrometer for accurate mass measurements.

Isolation of *C. forskohlii* Root Cork Oil Bodies

For isolation of oil bodies from root cork tissue, approximately 15 g of tissue was gently ground in 100 mL extraction buffer (20 mM Tricine, 250 mM Suc, 0.2 mM phenylmethylsulfonyl fluoride, pH 8.5); the homogenate was filtered through Miracloth (Calbiochem) and centrifuged at 3,500 rpm for 10 min for separation of cellular debris. The supernatant was collected and transferred in centrifugation tubes. Buffer B (20% [v/v] Suc, 20 mM HEPES, 100 mM KCl, 2 mM $MgCl_2$, pH 10.5) was overlaid (5 mL of B for 25 mL of supernatant), and samples were centrifuged for 40 min at 5,000*g*. The resulting floating oil bodies were collected carefully from the surface layer.

Identification and Cloning of Full-Length diTPS Genes

Mining of the *C. forskohlii* databases was performed as previously described (Zerbe et al., 2013) using tBLASTn software and known angiosperm diTPSs as query (CPS and EKS) and guided full-length cloning of a number of putative class I and class II diTPS genes. Total RNA from *C. forskohlii* roots, extracted as previously described (Hamberger et al., 2011), was used for cDNA synthesis. First-strand cDNA was synthesized using the Takara PrimeScript First-Strand cDNA Synthesis Kit and oligo(dT) primer. Cloning of the putative diTPS genes was achieved after PCR amplification using gene-specific primers that were designed based on the in silico sequences of the identified CfTPS genes (Supplemental Table S1). PCR products were cloned into the pJET1.2 vector and verified by sequencing.

Phylogenetic Analysis

The phylogenetic analyses are based on manually inspected amino acid alignments (DIALIGN-TX), which were analyzed by PhyML 3.1 (four rate substitution categories, Lee and Gascuel amino acid replacement matrix [LG substitution model], BIONJ starting tree, 100 bootstrap repetitions) and visualization in treeview (rooted with the bifunctional copalyl diphosphate synthase/kaurene synthase from the moss *Physcomitrella patens* PpCPS/EKS [BAF61135]). The abbreviations and accession numbers of sequences used are given in Supplemental Table S2.

RNA Extraction and Quantitative Real-Time PCR

Total RNA from *C. forskohlii* root cork was extracted according to Hamberger et al. (2011) and further purified using the Spectrum Plant Total RNA Kit (Sigma), while total RNA from leaves, flowers, stems, and root cortex and stele was extracted using the Spectrum Plant Total RNA Kit. RNA extraction was followed by on-column DNase I digestion. The integrity of RNA samples was evaluated using the RNA-nano assay on the Agilent 2100 Bioanalyzer (Agilent Technologies). First-strand cDNAs were synthesized from 0.5 μg of total RNA, with oligo(dT) primer, using the SuperScript III First-Strand Synthesis System for RT-PCR (Invitrogen). The resulting cDNA was diluted 10-fold for the quantitative reverse transcription-PCR reactions. The absence of genomic DNA contamination was verified by primers designed in exon-intron spanning regions of the Translation Initiation Factor4a (TIF4a) and Elongation Factor1a (EF1a) reference genes. Quantitative real-time PCR reactions were performed with gene-specific primers (Supplemental Table S1) and Maxima SYBR Green/Fluorescein qPCR Master Mix (Fermentas) on a Rotor-Gene Q cycler (Qiagen). The PCR reactions were performed using the following cycling parameters: 95°C for 7 min (enzyme activation), 35 cycles of 95°C for 15 s, 60°C for 30 s, and 72°C for 30 s, followed by a melting curve cycle from 60°C to 90°C. TIF4a and EF1a were used as reference genes as they showed the lowest variation across different tissues. No statistically significant differences were observed between the results obtained from the two different reference genes. The results were normalized with TIF4a. Relative transcript abundance was calculated as the mean of three biological replications (three different plants), while the reactions were performed in three technical replicates. Amplification efficiency was calculated with the Real Time PCR Miner (http://www.miner.ewindup.info/). Efficiency-corrected differential cycles over threshold for target to reference values were used to quantify relative differences in target gene transcript accumulation. Primer specificity was assessed by agarose gel analysis and sequencing of amplicons from representative reactions, as well as from melting curve analysis of every reaction.

Functional Characterization of CfTPS: In Vitro Assays

For the expression of the CfTPS1, CfTPS2, CfTPS3, CfTPS4, and CfTPS14 in *Escherichia coli*, pseudomature variants lacking predicted plastidial target sequences were cloned into the pET28b+ vector. The software ChloroP was used for prediction of the plastidial target sequence (http://www.cbs.dtu.dk/services/ChloroP/; Emanuelsson et al., 1999). As the expression levels of the recombinant CfTPS3 was very poor, a codon-optimized version was synthesized by GenScript USA and subsequently cloned into the same vector (sequence is given in Supplemental Table S3). pET28b+ constructs were transformed into *E. coli* BL-21DE3-C41 cells and inoculated in a starter culture with lysogeny broth media and 50 μg mL^{-1} kanamycin. A starter culture was diluted 1:100 in a 50 mL terrific broth medium with 50 μg mL^{-1} kanamycin and grown at 37°C and 180 rpm until the optical density at 600 nm reached 0.3 to 0.4. Cultures were cooled to 16°C, and expression was induced at optical density at 600 nm of approximately 0.6 with 0.2 mM isopropylthio-β-galactoside. Expression was done overnight, and cells were harvested by centrifugation. Binding buffer (20 mM HEPES, pH 7.5, 0.5 M NaCl, 25 mM Imidazole, 5% [v/v] glycerol), one protease inhibitor cocktail tablet per 100 mL (Roche), and 0.1 mg L^{-1} lysozyme were added to the cell pellet, which was gently shaken for 30 min and subsequently lysed by sonication (Branson sonifier 250; duty cycle, 30%; output control, 2–3; 1/4″ tip). The cell lysate was centrifuged for 25 min at 12,000*g*, and the supernatant was subsequently used for purification of the recombinant proteins. Proteins encoded by *C. forskohlii* diTPS and the characterized monoterpene cineole

synthase from Greek sage (*Salvia fruticosa* [SfCIN]; Kampranis et al., 2007) were purified on 1-mL His SpinTrap columns (GE Healthcare) using elution buffer (binding buffer with 325 mM Imidazole and 5 mM dithiothreitol [DTT]) and desalted on PD MiniTrap G-25 columns (GE Healthcare) with a desalting buffer (20 mM HEPES, pH 7.2, 350 mM NaCl, 5 mM DTT, 1 mM $MgCl_2$, 5% [v/v] glycerol). In vitro TPS assays were performed by adding 15 μM GGPP or GPP and 100 μg purified CfTPS (or SfCIN) enzymes in 397 μL enzyme assay buffer (50 mM HEPES, pH 7.2, 7.5 mM $MgCl_2$, 5% [v/v] glycerol, 5 mM DTT). Onto the reaction mix, 500 μL *n*-hexane (Fluka GC-MS grade) was gently added as an overlay. Assays were incubated for 60 min at 30°C and approximately 70 rpm, and the hexane overlay was subsequently removed for GC-MS analysis.

Functional Characterization of CfTPS: Transient Expression in *Nicotiana benthamiana*

Full-length CfTPS cDNAs were cloned into the *Agrobacterium tumefaciens* binary vector for plant transformation pCAMBIA1300_35Su with gene-specific primers (Supplemental Table S1) by USER cloning described in Nour-Eldin et al. (2006). Transient expression of *CfTPS* genes with the gene-silencing suppressor p19 protein (Voinnet et al., 2003) in *N. benthamiana* leaves and extraction of diterpenes were performed as recently described (Spanner et al., 2013). Hexane extracts of *N. benthamiana* expressing the gene-silencing suppressor p19 protein alone were used as controls. Compounds of interest were identified by comparison of GC-MS total ion chromatogram and extracted ion chromatograms (EICs) of mass-to-charge ratio (*m/z*) 275 and 272 from samples. The ion *m/z* 275 is characteristic of several labdane-type diterpenes, including manoyl oxide, whereas *m/z* 272 is characteristic of several other nonlabdane-type diterpenes such as abietane-like diterpenes. All extractions from *N. benthamiana* transiently expressing diTPSs were carried out in biological triplicates (different leaves per plants infiltrated with the same agrobacteria mixture).

Metabolite Analysis from in Vitro and in Planta Assays

For the GC-MS analysis of *N. benthamiana* leaves expressing the CfTPSs and specific *C. forskohlii* tissues, 500 μL GC-MS-grade hexane were added to two leaf discs (diameter = 3 cm) in a 1.5-mL glass vial. Samples were incubated at room temperature for 1 h in a Roto-Shake Genie revolving at 40 cycles min^{-1}. After extraction, the solvent was transferred into new 1.5-mL glass vials and stored at –20°C until GC-MS analysis. One microliter of hexane extract was injected into a Shimadzu GC-MS-QP2010 Ultra. Separation was carried out using an Agilent HP-5MS column (30-m × 0.250-mm i.d., 0.25-μm film thickness) with purge flow of 1 mL min^{-1}, using helium as carrier gas. The GC temperature program was 50°C for 2 min, ramp at rate 4°C min^{-1} to 110°C, ramp at rate 8°C min^{-1} to 250°C, ramp at rate 10°C min^{-1} to 310°C, and hold for 5 min. Injection temperature was set at 250°C in splitless mode. For the GC-MS analysis of hexane extracts from in vitro assay, the following GC-program was used: 100°C for 1 min, ramp at rate 10°C min^{-1} to 250°C, ramp at rate 20°C min^{-1} to 310°C, and hold for 2 min. Compound identification was done by comparison to authentic standards (dehydroabietadiene, abietadiene), reference spectra from literature, databases, and comparison of retention time (miltiradiene, manoyl oxide, copalol, labd-13-en-8,15-diol and 13[16]-14-labdien-8-ol; John Wiley and Sons, 2006; Adams, 2007; Lane et al., 2010;). The differentiation of the C-13 epimers (13R) and (13S) manoyl oxide was performed as previously described (Demetzos et al., 2002). For the GC-MS analysis of hexane extracts from in vitro assays using GPP as substrate, the parameters used were: 2 min at 50°C, ramp to 140°C with 20°C min^{-1}, ramp to 320°C with 10°C min^{-1} to 320°C, and hold for 3 min. One microliter was injected in splitless mode at 250°C, and the system was set in constant velocity mode with a linear velocity of 59.8 cm sec^{-1} using H_2 as carrier gas. Solvent cutoff was set to 3.5 min.

Sequence data from this article have been submitted to the GenBank/EBI Data Bank under the following accession numbers KF444506 (CfTPS1), KF444507 (CfTPS2), KF444508 (CfTPS3), KF444509 (CfTPS4), and KF471011 (CfTPS15).

Supplemental Data

The following materials are available in the online version of this article.

Supplemental Figure S1. Bright field microscopy of *C. forskohlii* stem cross section.

Supplemental Figure S2. Alignment of the CfTPSs protein sequences together with PpCPS/EKS.

Supplemental Figure S3. GC-MS analysis of hexane extract from in vitro assays using GPP as substrate.

Supplemental Table S1. List of primers used in this study.

Supplemental Table S2. Annotation and GenBank accession numbers of the proteins used in the phylograms.

Supplemental Table S3. Alignment of the nucleotide sequences of the native CfTPS3 (natCfTPS3) and the synthetic variant (synCfTPS3).

ACKNOWLEDGMENTS

We thank Dr. Damian Drew (University of Copenhagen, Faculty of Science, Department of Plant and Environmental Sciences) for critical reading of the manuscript, Dr. Carl Erik Olsen (University of Copenhagen, Faculty of Science, Department of Plant and Environmental Sciences) for excellent technical assistance with the LC-MS metabolomics, the green house service personnel of the University of Copenhagen, Faculty of Science, Department of Plant and Environmental Sciences, and Jason Goodger (University of Melbourne, School of Botany) for providing a clone of SfCIN.

Received September 12, 2013; accepted January 30, 2014; published January 30, 2014.

LITERATURE CITED

Adams RP (2007) Identification of Essential Oil Components by Gas Chromatography/Mass Spectrometry, Ed 4th. Allured Publishing Corporation, Carol Stream, Illinois

Alasbahi RH, Melzig MF (2010a) *Plectranthus barbatus*: a review of phytochemistry, ethnobotanical uses and pharmacology: part 1. Planta Med **76:** 653–661

Alasbahi RH, Melzig MF (2010b) *Plectranthus barbatus*: a review of phytochemistry, ethnobotanical uses and pharmacology: part 2. Planta Med **76:** 753–765

Ammon HP, Müller AB (1985) Forskolin: from an ayurvedic remedy to a modern agent. Planta Med **51:** 473–477

Angelopoulou D, Demetzos C, Dimas C, Perdetzoglou D, Loukis A (2001) Essential oils and hexane extracts from leaves and fruits of *Cistus monspeliensis*. Cytotoxic activity of *ent*-13-epi-manoyl oxide and its isomers. Planta Med **67:** 168–171

Asada Y, Li W, Terada T, Kuang X, Li Q, Yoshikawa T, Hamaguchi S, Namekata I, Tanaka H, Koike K (2012) Labdane-type diterpenoids from hairy root cultures of *Coleus forskohlii*, possible intermediates in the biosynthesis of forskolin. Phytochemistry **79:** 141–146

Beller M, Thiel K, Thul PJ, Jäckle H (2010) Lipid droplets: a dynamic organelle moves into focus. FEBS Lett **584:** 2176–2182

Bhat SV, Bajqwa BS, Dornauer H, do Scusa NJ, Fehlhaber HW (1977) Structures and stereochemistry of new labdane diterpiniods from *Coleus forskohlii* briq. Tetrahedron Lett **18:** 1669–1672

Caniard A, Zerbe P, Legrand S, Cohade A, Valot N, Magnard JL, Bohlmann J, Legendre L (2012) Discovery and functional characterization of two diterpene synthases for sclareol biosynthesis in *Salvia sclarea* (L.) and their relevance for perfume manufacture. BMC Plant Biol **12:** 119

Chapman KD, Dyer JM, Mullen RT (2012) Biogenesis and functions of lipid droplets in plants. Thematic review series. Lipid droplet synthesis and metabolism: from yeast to man. J Lipid Res **53:** 215–226

Chatzopoulou FM, Makris AM, Argiriou A, Degenhardt J, Kanellis AK (2010) EST analysis and annotation of transcripts derived from a trichome-specific cDNA library from *Salvia fruticosa*. Plant Cell Rep **29:** 523–534

Chen F, Tholl D, Bohlmann J, Pichersky E (2011) The family of terpene synthases in plants: a mid-size family of genes for specialized metabolism that is highly diversified throughout the kingdom. Plant J **66:** 212–229

da Silva LL, Nascimento MS, Cavalheiro AJ, Silva DH, Castro-Gamboa I, Furlan M, Bolzani VdaS (2008) Antibacterial activity of labdane diterpenoids from *Stemodia foliosa*. J Nat Prod **71:** 1291–1293

Daly JW (1984) Forskolin, adenylate cyclase, and cell physiology: an overview. Adv Cyclic Nucleotide Protein Phosphorylation Res **17:** 81–89

de las Heras B, Hoult JR (1994) Non-cytotoxic inhibition of macrophage eicosanoid biosynthesis and effects on leukocyte functions and reactive oxygen species of two novel anti-inflammatory plant diterpenoids. Planta Med **60:** 501–506

De Vos RC, Moco S, Lommen A, Keurentjes JJ, Bino RJ, Hall RD (2007) Untargeted large-scale plant metabolomics using liquid chromatography coupled to mass spectrometry. Nat Protoc **2:** 778–791

Demetzos C, Kolocouris A, Anastasaki T (2002) A simple and rapid method for the differentiation of C-13 manoyl oxide epimers in biologically important samples using GC-MS analysis supported with NMR spectroscopy and computational chemistry results. Bioorg Med Chem Lett **12:** 3605–3609

Demetzos C, Mitaku S, Couladis M, Harvala C, Kokkinopoulos D (1994) Natural metabolites of *ent*-13-epi-manoyl oxide and other cytotoxic diterpenes from the resin "LADANO" of *Cistus creticus*. Planta Med **60:** 590–591

Diaz G, Melis M, Batetta B, Angius F, Falchi AM (2008) Hydrophobic characterization of intracellular lipids in situ by Nile Red red/yellow emission ratio. Micron **39:** 819–824

Dimas K, Demetzos C, Mitaku S, Vaos B, Marselos M, Tzavaras T, Kokkinopoulos D (1999) Cytotoxic activity and antiproliferative effects of a new semi-synthetic derivative of *ent*-3 β-hydroxy-13-epi-manoyl oxide on human leukemic cell lines. Anticancer Res **19**(5B): 4065–4072

Eltgroth ML, Watwood RL, Wolfe GV (2005) Production and cellular localization of neutral long-chain lipids in the haptophyte algae *Isochrysis galban*a and *Emiliania huxleyi*. J Phycol **41:** 1000–1009

Emanuelsson O, Nielsen H, von Heijne G (1999) ChloroP, a neural network-based method for predicting chloroplast transit peptides and their cleavage sites. Protein Sci **8:** 978–984

Falara V, Pichersky E, Kanellis AK (2010) A copal-8-ol diphosphate synthase from the angiosperm *Cistus creticus* subsp. *creticus* is a putative key enzyme for the formation of pharmacologically active, oxygen-containing labdane-type diterpenes. Plant Physiol **154:** 301–310

Ferreres F, Figueiredo R, Bettencourt S, Carqueijeiro I, Oliveira J, Gil-Izquierdo A, Pereira DM, Valentão P, Andrade PB, Duarte P, et al (2011) Identification of phenolic compounds in isolated vacuoles of the medicinal plant *Catharanthus roseus* and their interaction with vacuolar class III peroxidase: an H_2O_2 affair? J Exp Bot **62:** 2841–2854

Fragoso-Serrano M, González-Chimeo E, Pereda-Miranda R (1999) Novel labdane diterpenes from the insecticidal plant *Hyptis spicigera*. J Nat Prod **62:** 45–50

Fujimoto T, Parton RG (2011) Not just fat: the structure and function of the lipid droplet. Cold Spring Harb Perspect Biol **3:** 3

Gao W, Hillwig ML, Huang L, Cui G, Wang X, Kong J, Yang B, Peters RJ (2009) A functional genomics approach to tanshinone biosynthesis provides stereochemical insights. Org Lett **11:** 5170–5173

Gershenzon J, Dudareva N (2007) The function of terpene natural products in the natural world. Nat Chem Biol **3:** 408–414

Gershenzon J, McConkey ME, Croteau RB (2000) Regulation of monoterpene accumulation in leaves of peppermint. Plant Physiol **122:** 205–214

Guo J, Zhou YJ, Hillwig ML, Shen Y, Yang L, Wang Y, Zhang X, Liu W, Peters RJ, Chen X, et al (2013) CYP76AH1 catalyzes turnover of miltiradiene in tanshinones biosynthesis and enables heterologous production of ferruginol in yeasts. Proc Natl Acad Sci USA **110:** 12108–12113

Habibi Z, Eftekhar F, Samiee K, Rustaiyan A (2000) Structure and antibacterial activity ofp6 new labdane diterpenoid from *Salvia leriaefolia*. J Nat Prod **63:** 270–271

Hamberger B, Bak S (2013) Plant P450s as versatile drivers for evolution of species-specific chemical diversity. Philos Trans R Soc Lond B Biol Sci **368:** 20120426

Hamberger B, Ohnishi T, Hamberger B, Séguin A, Bohlmann J (2011) Evolution of diterpene metabolism: Sitka spruce CYP720B4 catalyzes multiple oxidations in resin acid biosynthesis of conifer defense against insects. Plant Physiol **157:** 1677–1695

Hayashi KI, Horie K, Hiwatashi Y, Kawaide H, Yamaguchi S, Hanada A, Nakashima T, Nakajima M, Mander LN, Yamane H, et al (2010) Endogenous diterpenes derived from *ent*-kaurene, a common gibberellin precursor, regulate protonema differentiation of the moss *Physcomitrella patens*. Plant Physiol **153:** 1085–1097

He X, Sun Y, Zhu RL (2013) The oil bodies of liverworts: unique and important organelles in land plants. Crit Rev Plant Sci **32:** 293–302

Heskes AM, Goodger JQ, Tsegay S, Quach T, Williams SJ, Woodrow IE (2012) Localization of oleuropeyl glucose esters and a flavanone to secretory cavities of Myrtaceae. PLoS ONE **7:** e40856

Hurley JH (1998) The adenylyl and guanylyl cyclase superfamily. Curr Opin Struct Biol **8:** 770–777

Iijima Y, Davidovich-Rikanati R, Fridman E, Gang DR, Bar E, Lewinsohn E, Pichersky E (2004) The biochemical and molecular basis for the divergent patterns in the biosynthesis of terpenes and phenylpropenes in the peltate glands of three cultivars of basil. Plant Physiol **136:** 3724–3736

John Wiley and Sons (2006) Wiley Registry of Mass Spectral Data, Ed 8 for Windows [CD ROM]. John Wiley and Sons, Hoboken, NJ

Kampranis SC, Ioannidis D, Purvis A, Mahrez W, Ninga E, Katerelos NA, Anssour S, Dunwell JM, Degenhardt J, Makris AM, et al (2007) Rational conversion of substrate and product specificity in a *Salvia* monoterpene synthase: structural insights into the evolution of terpene synthase function. Plant Cell **19:** 1994–2005

Kavitha C, Rajamani K, Vadivel E (2010) *Coleus forskohlii*: a comprehensive review on morphology, phytochemistry and pharmacological aspects. J Med Plant Res **4:** 278–285

Keeling CI, Dullat HK, Yuen M, Ralph SG, Jancsik S, Bohlmann J (2010) Identification and functional characterization of monofunctional *ent*-copalyl diphosphate and *ent*-kaurene synthases in white spruce reveal different patterns for diterpene synthase evolution for primary and secondary metabolism in gymnosperms. Plant Physiol **152:** 1197–1208

Keeling CI, Weisshaar S, Ralph SG, Jancsik S, Hamberger B, Dullat HK, Bohlmann J (2011) Transcriptome mining, functional characterization, and phylogeny of a large terpene synthase gene family in spruce (*Picea* spp.). BMC Plant Biol **11:** 43

Kelecom A (1983) Isolation, structure determination, and absolute configuration of barbatusol, a new bioactive diterpene with a rearranged abietane skeleton from the labiate *Coleus barbatus*. Tetrahedron **39:** 3603–3608

Kelecom A (1984) An abietane diterpene from the labiate *Coleus barbatus*. Phytochemistry **23:** 1677–1679

Kikura M, Morita K, Sato S (2004) Pharmacokinetics and a simulation model of colforsin daropate, new forskolin derivative inotropic vasodilator, in patients undergoing coronary artery bypass grafting. Pharmacol Res **49:** 275–281

Lane A, Boecklemann A, Woronuk GN, Sarker L, Mahmoud SS (2010) A genomics resource for investigating regulation of essential oil production in *Lavandula angustifolia*. Planta **231:** 835–845

Li JL, Chen QQ, Jin QP, Gao J, Zhao PJ, Lu S, Zeng Y (2012a) IeCPS2 is potentially involved in the biosynthesis of pharmacologically active *Isodon* diterpenoids rather than gibberellin. Phytochemistry **76:** 32–39

Li Z, Tang T, Liang S, Ning X, Bai M, Wu H (2012b) The synthesis and storage sites of phenolic compounds in the root and rhizome of *Echinacea purpurea*. Am J Plant Sci **3:** 551–558

Li Z, Wang J (2006) A forskolin derivative, FSK88, induces apoptosis in human gastric cancer BGC823 cells through caspase activation involving regulation of Bcl-2 family gene expression, dissipation of mitochondrial membrane potential and cytochrome c release. Cell Biol Int **30:** 940–946

Lukhoba CW, Simmonds MS, Paton AJ (2006) Plectranthus: a review of ethnobotanical uses. J Ethnopharmacol **103:** 1–24

Mahlberg P (1993) Laticifers: An historical perspective. Bot Rev **59:** 1–23

Marinova K, Kleinschmidt K, Weissenböck G, Klein M (2007) Flavonoid biosynthesis in barley primary leaves requires the presence of the vacuole and controls the activity of vacuolar flavonoid transport. Plant Physiol **144:** 432–444

Martin D, Tholl D, Gershenzon J, Bohlmann J (2002) Methyl jasmonate induces traumatic resin ducts, terpenoid resin biosynthesis, and terpenoid accumulation in developing xylem of Norway spruce stems. Plant Physiol **129:** 1003–1018

Morant AV, Jørgensen K, Jørgensen C, Paquette SM, Sánchez-Pérez R, Møller BL, Bak S (2008) β-Glucosidases as detonators of plant chemical defense. Phytochemistry **69:** 1795–1813

Morrone D, Hillwig ML, Mead ME, Lowry L, Fulton DB, Peters RJ (2011) Evident and latent plasticity across the rice diterpene synthase family with potential implications for the evolution of diterpenoid metabolism in the cereals. Biochem J **435:** 589–595

Murphy DJ (2012) The dynamic roles of intracellular lipid droplets: from archaea to mammals. Protoplasma **249:** 541–585

Nour-Eldin HH, Hansen BG, Nørholm MH, Jensen JK, Halkier BA (2006) Advancing uracil-excision based cloning towards an ideal technique for cloning PCR fragments. Nucleic Acids Res **34:** e122

Penno A, Hackenbroich G, Thiele C (2013) Phospholipids and lipid droplets. Biochim Biophys Acta **1831:** 589–594

Peters RJ (2006) Uncovering the complex metabolic network underlying diterpenoid phytoalexin biosynthesis in rice and other cereal crop plants. Phytochemistry **67:** 2307–2317

Peters RJ (2010) Two rings in them all: the labdane-related diterpenoids. Nat Prod Rep **27:** 1521–1530

Post J, van Deenen N, Fricke J, Kowalski N, Wurbs D, Schaller H, Eisenreich W, Huber C, Twyman RM, Prüfer D, et al (2012) Laticifer-specific cis-prenyltransferase silencing affects the rubber, triterpene, and inulin content of *Taraxacum brevicorniculatum*. Plant Physiol **158:** 1406–1417

Ro DK, Arimura GI, Lau SY, Piers E, Bohlmann J (2005) Loblolly pine abietadienol/abietadienal oxidase PtAO (CYP720B1) is a multifunctional, multisubstrate cytochrome P450 monooxygenase. Proc Natl Acad Sci USA **102:** 8060–8065

Rodríguez-Concepción M, Boronat A (2002) Elucidation of the methylerythritol phosphate pathway for isoprenoid biosynthesis in bacteria and plastids. A metabolic milestone achieved through genomics. Plant Physiol **130:** 1079–1089

Sallaud C, Giacalone C, Töpfer R, Goepfert S, Bakaher N, Rösti S, Tissier A (2012) Characterization of two genes for the biosynthesis of the labdane diterpene Z-abienol in tobacco (*Nicotiana tabacum*) glandular trichomes. Plant J **72:** 1–17

Schilmiller AL, Last RL, Pichersky E (2008) Harnessing plant trichome biochemistry for the production of useful compounds. Plant J **54:** 702–711

Seamon KB, Padgett W, Daly JW (1981) Forskolin: unique diterpene activator of adenylate cyclase in membranes and in intact cells. Proc Natl Acad Sci USA **78:** 3363–3367

Siebert DJ (2004) Localization of salvinorin A and related compounds in glandular trichomes of the psychoactive sage, *Salvia divinorum*. Ann Bot (Lond) **93:** 763–771

Silvestro D, Andersen TG, Schaller H, Jensen PE (2013) Plant sterol metabolism. Δ^7-Sterol-C_5-desaturase (STE1/DWARF7), $\Delta^{5,7}$-sterol-Δ^7-reductase (DWARF5) and Δ^{24}-sterol-Δ^{24}-reductase (DIMINUTO/DWARF1) show multiple subcellular localizations in *Arabidopsis thaliana* (Heynh) L. PLoS ONE **8:** e56429

Sirikantaramas S, Yamazaki M, Saito K (2008) Mechanisms of resistance to self-produced toxic secondary metabolites in plants. Phytochem Rev **7:** 467–477

Spanner SB, Bassard JÉ, Andersen-Ranberg J, Møldrup ME, Simonsen HT, Hamberger B (2014) High throughput testing of terpenoid biosynthesis candidate genes using transient expression in *Nicotiana benthamiana*. *In* M Rodríguez Concepción, ed, Plant Isoprenoids, Methods in Molecular Biology, Vol. 1153. Humana Press, New York (in press)

Swaminathan S, Morrone D, Wang Q, Fulton DB, Peters RJ (2009) CYP76M7 is an *ent*-cassadiene C11α-hydroxylase defining a second multifunctional diterpenoid biosynthetic gene cluster in rice. Plant Cell **21:** 3315–3325

Toya Y, Schwencke C, Ishikawa Y (1998) Forskolin derivatives with increased selectivity for cardiac adenylyl cyclase. J Mol Cell Cardiol **30:** 97–108

Uribe S, Ramirez J, Peña A (1985) Effects of β-pinene on yeast membrane functions. J Bacteriol **161:** 1195–1200

Valdés LJ III, Mislankar SG, Paul AG (1987) *Coleus barbatus* (*C. forskohlii*) (Lamiaceae) and the potential new drug forskolin (coleonol). Econ Bot **41:** 474–483

Voinnet O, Rivas S, Mestre P, Baulcombe D (2003) An enhanced transient expression system in plants based on suppression of gene silencing by the p19 protein of tomato bushy stunt virus. Plant J **33:** 949–956

Voo SS, Grimes HD, Lange BM (2012) Assessing the biosynthetic capabilities of secretory glands in citrus peel. Plant Physiol **159:** 81–94

Wagh K, Patil P, Surana S, Wagh V (2012) Forskolin: upcoming antiglaucoma molecule. J Postgrad Med **58:** 199–202

Wang Q, Hillwig ML, Peters RJ (2011) CYP99A3: functional identification of a diterpene oxidase from the momilactone biosynthetic gene cluster in rice. Plant J **65:** 87–95

Xie Z, Kapteyn J, Gang DR (2008) A systems biology investigation of the MEP/terpenoid and shikimate/phenylpropanoid pathways points to multiple levels of metabolic control in sweet basil glandular trichomes. Plant J **54:** 349–361

Xu LL, Lu J, Li WJ, Kong LY (2005) Studies on the chemical constituents in root of *Coleus forskohlii*. Zhongguo Zhong Yao Za Zhi **30:** 1753–1755

Ye H, Deng G, Liu J, Qiu FG (2009) Expedient construction of the Ziegler intermediate useful for the synthesis of forskolin via consecutive rearrangements. Org Lett **11:** 5442–5444

Yoneyama M, Sugiyama A, Satoh Y, Takahara A, Nakamura Y, Hashimoto K (2002) Cardiovascular and adenylate cyclase stimulating effects of colforsin daropate, a water-soluble forskolin derivative, compared with those of isoproterenol, dopamine and dobutamine. Circ J **66:** 1150–1154

Zerbe P, Chiang A, Yuen M, Hamberger B, Hamberger B, Draper JA, Britton R, Bohlmann J (2012) Bifunctional cis-abienol synthase from *Abies balsamea* discovered by transcriptome sequencing and its implications for diterpenoid fragrance production. J Biol Chem **287:** 12121–12131

Zerbe P, Hamberger B, Yuen MM, Chiang A, Sandhu HK, Madilao LL, Nguyen A, Hamberger B, Bach SS, Bohlmann J (2013) Gene discovery of modular diterpene metabolism in nonmodel systems. Plant Physiol **162:** 1073–1091

Zhao J, Huhman D, Shadle G, He XZ, Sumner LW, Tang Y, Dixon RA (2011) MATE2 mediates vacuolar sequestration of flavonoid glycosides and glycoside malonates in *Medicago truncatula*. Plant Cell **23:** 1536–1555

Zore GB, Thakre AD, Jadhav S, Karuppayil SM (2011) Terpenoids inhibit *Candida albicans* growth by affecting membrane integrity and arrest of cell cycle. Phytomedicine **18:** 1181–1190

Zulak KG, Bohlmann J (2010) Terpenoid biosynthesis and specialized vascular cells of conifer defense. J Integr Plant Biol **52:** 86–97